The Society shall not be responsible for statements or opinions advanced in papers or discussion at meetings of the Society or of its Divisions or Sections, or printed in its publications. Discussion is printed only if the paper is published in an ASME Journal. Authorization to photocopy material for internal or personal use under circumstance not falling within the fair use provisions of the Copyright Act is granted by ASME to libraries and other users registered with the Copyright Clearance Center (CCC) Transactional Reporting Service provided that the base fee of $0.30 per page is paid directly to the CCC, 27 Congress Street, Salem MA 01970. Requests for special permission or bulk reproduction should be addressed to the ASME Technical Publishing Department.

Copyright © 1997 by ASME All Rights Reserved Printed in U.S.A

HIGH FREESTREAM TURBULENCE SIMULATION IN A SCALED-UP TURBINE VANE PASSAGE

B. A. Bangert, A. Kohli, J. H. Sauer, and K. A. Thole
Mechanical Engineering Department
University of Wiscsonsin
Madison, Wisconsin 53706

Abstract

Quantifying high freestream turbulence effects on surface heat transfer and on blade boundary layer development is important for improving predictions of the thermal loading and aerodynamic losses for gas turbine blades, vanes, and endwalls. To improve our physical understanding as well as improve CFD capabilities, detailed flow and thermal field data is needed in addition to surface data. This paper discusses the development of a turbulence generator that is capable of generating turbulence intensities as high as 20% and yet allow an independent control on the turbulent length scale. The integral length scale at a turbulence intensity of TI = 20% ranged from 2.1 cm to 5.5 cm. The development of the turbulence generator took place in a wind tunnel having a large, constant area, test section. After this development, the turbulence generator was placed upstream of a scaled-up turbine vane. This paper also describes the development of the turbine vane test section that has a central first stage stator vane that was scaled up by a factor of nine. Finally, turbulence measurements, turbulent length scales, and energy spectra measured inside the turbine vane passage are presented and compared to measurements that were made in the constant area test section. The results indicate that in the first 40% of the stator vane passage, the turbulence levels rapidly decrease by a factor of four with the integral length scales having a rapid growth.

Introduction

Predicting the thermal loading and aerodynamic losses for turbine components has been and continues to be of primary importance to the gas turbine industry. One prominent effect that plagues this predictive capability is the role of high turbulence levels. Typical turbulence levels exiting the combustor are as high as 20% (Kuotmos and McGuirk, 1989). Numerous flat plate studies have shown that increases in surface heat transfer are a function of both turbulent length scale as well as turbulence intensities. Although there have been relatively fewer turbine vane studies than flat plate studies in which there has been a systematic variation of turbulence intensity and length scale, the results consistently show the importance of both turbulent length scale and level on surface heat transfer.

There are three objectives for this paper. First, this paper describes a method for generating freestream turbulence in a large cross-sectional wind tunnel area that have levels as high as TI = 20% with a relatively uniform mean velocity field and with a length scale that can be independently controlled. Note that there are now a number of different high freestream turbulence generators that have been presented in the literature that are able to produce high turbulence intensities, but these devices have not allowed for an independent control of the turbulent length scale. Second, this paper describes a new facility having a turbine vane test section that consists of a modern-day stator vane that is scaled up by a factor of nine in which engine Reynolds numbers are matched. Third, this paper presents measurements of the turbulence level decay, energy spectra, and turbulent length scale growths inside the passage of the scaled-up stator vane. The turbulence decay and length scale growths occurring in the turbine passages are subjected to curvature and acceleration effects as compared to that occurring in a constant area test section. The decays and growths inside the turbine passage will be compared to those occurring in a constant cross-sectional area. Although past turbine airfoil studies have investigated high turbulence level effects on surface heat transfer, these studies have for the most part only reported incoming turbulence intensities and length scales.

The following sections describe relevant past studies, the experimental facility and measurement techniques used for this study, the development of the turbulence generator, a description of the turbine vane geometry, and finally the turbulence decay, energy spectra, and length scale growths in the turbine vane passage.

Past Studies

Past studies have indicated the importance of turbulent length scale and turbulence level on scaling the surface heat transfer. As pointed out by Thole and Bogard (1992), increases in surface heat transfer for flat plate applications best scale with a TLR parameter first developed by Ames and Moffat (1990). The TLR parameter, defined as $TLR = TI\,(\Delta 2/L_u)^{0.33}\,(Re_{\Delta 2}/1000)^{0.25}$, is a function of both turbulence level and length scale . This section discusses recent turbine blade heat transfer studies, methods available for generating high levels of freestream turbulence

Presented at the International Gas Turbine & Aeroengine Congress & Exhibition
Orlando, Florida — June 2–June 5, 1997

levels, as well as some relevant studies on streamwise variations of turbulence characteristics in passages having varying cross sections.

One recent study addressing grid-generated freestream turbulence affecting surface heat transfer on a turbine vane is that of Hoffs, Drost, and Bölcs (1996). Hoffs, et al. compared heat transfer coefficients for a range of Reynolds numbers at a turbulence intensity of TI = 5.5% and 11% and length scales of Λ_x = 25 mm and 13 mm, respectively. As expected, the most pronounced effect of the turbulence intensity was to move the transition location closer to the stagnation region on the suction surface. At the low Reynolds numbers (Re < 730,000), the effect of increasing the turbulence intensity from 5.5% to 11%, results in an increase in the heat transfer coefficient by as much as 20% on the pressure side. At higher Reynolds numbers of 1×10^5, transition from laminar to turbulent becomes much more apparent at TI = 11% on the pressure surface. Hoff, et al. did not, however, present any measurements documenting the turbulence characteristics inside the passage.

The study presented by Ames (1995) is the only study which investigates two distinctly different dissipation length scales, L_u = 1.36 cm and L_u = 4.26 cm, at nominally the same freestream turbulence level of TI = 8%. Ames also presented a higher turbulence intensity case of TI = 12% with a length scale of L_u = 3.36 cm. Note that the two studies with the larger length scales (L_u = 4.26 and 3.36 cm) used a combustor simulator upstream of a linear cascade to generate the turbulence intensities whereas the small length scale study used a grid. The surface heat transfer measurements showed that on the suction surface, early transition was induced due to the high turbulence intensity. Although the Stanton number increases along the turbulent portion of the suction side of the vane, there is no effect of length scale and only a small effect due to freestream turbulence. Data for the pressure side, however, indicated a much larger increase in heat transfer (60%) for the TI = 12% case. In addition, for the pressure side there was a distinct effect of length scale in that there was an increase in the surface heat transfer from 42% to 51% as the length scale was decreased from L_u = 4.26 cm to 1.36 cm at a TI ~ 8%.

Since the flow throughout a turbine vane passage experiences a strain rate, it would be quite surprising that the turbulence characteristics would be similar to those of isotropic, homogeneous turbulence decays which occur in constant flow areas. Therefore, there is a need to measure the turbulence decay and length scale growth inside the vane passage to compare the decay with that occurring in the case of homogeneous, isotropic turbulence decay. A comprehensive study by Tan-atichat, et al. (1980), who studied turbulence decays and length scale growths in axisymmetric contractions, showed that how the turbulence is altered by the contraction depends on the incoming turbulence scales, the total strain experienced by the flow, and the strain rate caused by the contraction. In addition, Tan-atichat, et al. showed that the transverse turbulence components are affected more than the streamwise components. Other than in a detailed report presented by Ames (1994), the development of the turbulence characteristics though a turbine vane passageway has not been documented for high freestream turbulence levels.

Several methods for generating turbulence, other than passive grids, have been reported in the literature with most of these methods appearing in more recent years. Recent turbulence generation methods can be broadly classified into wall jets (MacMullin, Elrod, and Rivir, 1989 and Maciejewski and Moffat, 1992); normal jet injection (Thole and Bogard, 1992); a combustor simulator (Ames, 1992); and active grids (Young, et al., 1992 and Sahm and Moffat, 1992). Although the Maciejewski and Moffat (1992) were able to achieve turbulence intensities as high as TI = 60%, the wall jets have the inherent problem of a non-uniform mean flowfield which makes it difficult to apply to a turbine vane geometry. The limiting factor for the normal jet injection is the ability for the jets-in-crossflow to penetrate to the centerline of large test sections. The normal jet injection method was used by Thole and Bogard (1992) in a wind tunnel having a small cross-sectional height (15.24 cm) and was able to achieve turbulence intensities as high as TI = 20% with a relatively uniform mean field. The method used by Ames (1990, 1994) in two different facilities has been a scaled-up combustor simulator that achieved turbulence intensities as high as TI = 13% (Ames, 1994) for his scaled-up vane studies. By adjusting the distance between the combustor simulator and the cascade inlet, Ames was able to simulate two length scales L_u = 3.36 cm and 4.34 cm at a TI ~ 8%.

There have been a number of active grid studies including early ones by Gad-El-Hak and Corrsin (1974), who used parallel bars, and Tassa and Kamotani (1975), who used a biplanar grid. Both of these early studies used evenly spaced holes placed in the surface of hollow rods to inject jets either in the upstream direction or in the downstream direction relative to the mainstream flow. Gad-El-Hak and Corrsin (1974) found that weak upstream injection could actually reduce the turbulence levels relative to a passive grid with no injection, but as the mass flux injection

Nomenclature

C	True chord length
D	Diameter of a turbulence generator element
D_{jet}	Turbulence generator jet hole diameter
d_w	Diameter of hot-wire sensor
E(k)	Energy spectra of streamwise velocity fluctuations
f	Frequency (1/s)
k	Wavenumber, $2\pi f/U_\infty$
K	Acceleration parameter, $K = \frac{\nu}{U_\infty^2}\frac{dU_\infty}{dx}$
L_u	Dissipation length scale, $L_u = 1.5\,\lvert u'^3\rvert / \varepsilon$
l_w	Length of hot-wire sensor
m	Exponent for integral length scale growth
MFR	Jet-to-mainstream mass flux ratio, equation (1)
n	Exponent for turbulence level decay
P_0	Stagnation pressure
p	Static pressure
Re_s	Vane Reynolds number based on surface distance
s	Surface distance along vane from stagnation
s_L	Lateral grid element spacing
s_V	Vertical jet hole spacing
TI	Streamwise turbulence intensity, u'/U_∞
TLR	Turbulence level scaling parameter
U_∞	Mainstream velocity in streamwise direction
U, u'	Mean, rms of fluctuating streamwise velocity
V, v'	Mean, rms of fluctuating lateral velocity
w	Turbine vane passage width normal to streamlines
x	Streamwise distance from turbulence generator
X	Vane coordinates
Y	Vane coordinates

Greek

Δ_2	Enthalpy thickness
ε	Turbulent dissipation, estimated from the following: $(18/55)\,A\,\varepsilon^{2/3}k^{-5/3}$, A = 1.62
Λ_x	Streamwise integral length scale
σ	Standard deviation

ratio is increased to above 5.5%, the turbulence levels begin to increase due to the additional shear in the jets themselves. For a given injection rate, higher turbulence levels occurred with upstream injection than downstream injection where the highest mass flux injection rate of 8% resulted in the highest turbulence level of TI =6% at a streamwise distance of 30 mesh widths. Tassa and Kamotani (1975), on the other hand found that for a fixed injection rate, higher turbulence levels occurred when injecting upstream from their biplanar grid rather than downstream. Much later, Young, et al. (1992) used injection from their grid of crossed rods in which they either injected upstream resulting in turbulence intensities as high as TI = 12% or injected downstream with turbulence intensities as high as TI = 25% at 20 grid diameters downstream. Sahm and Moffat (1992) injected at ±30° relative to the mainstream crossflow direction to obtain turbulence levels as high as 21% at a downstream location of 30 mesh widths. Using their same geometry, Sahm and Moffat were able to achieve only a TI = 13% with upstream injection alone.

Given the fact that the active jet grids looked the most promising in terms of generating high levels of freestream turbulence in relatively large cross-sectional flow areas, we began developing this type of generator with the hope of being able to independently control the length scale at a fixed turbulence level. Knowing that a grid can be used to generate different length scales depending on the geometry (Comte-Bellot and Corrsin, 1971), this study was also aimed at controlling the length scale through changes in the mesh geometry.

Experimental Facilities and Techniques

The primary facility used in this study was a closed-loop wind tunnel with two working test sections as shown in Figure 1. The air is driven through this wind tunnel using a 50 Hp fan with the rotation of the blades being controlled through a frequency modulator. The fan is followed by a heat exchanger section to control the temperature which is then followed by a 6.25:1 contraction. Downstream of the contraction is a primary test section that is 1.8 m long with a square cross-sectional area of 61 cm by 61 cm. The development of the turbulence generator took place in the primary test section. The background turbulence level in the primary test section (without the turbulence generator) is TI = 0.3%. Downstream of the primary test section is a diffuser that contains screens to again condition the flow which is followed by a corner test section. The cross-sectional area to work with at the start of the elbow is 1 m by 1 m. The scaled-up turbine vane was installed in this corner test section. For this corner test section, the area was reduced in the vertical direction to 59 cm in height using a contraction to insure that the scaled up span-to-chord ratio was matched to the real turbine vane.

Measurements involving the development of the turbulence generator included those of mean and fluctuating velocity, and length scales. The mean and fluctuating velocity measurements were measured with a two-component laser Doppler velocimeter (LDV) and a hot-wire anemometer. The LDV system included a TSI Model 9800 fiber-optic probe with a 5 W laser, Model 9201 Colorburst Multicolor beam separator, and a focusing lens with a focal length of 350 mm. Velocity data from the LDV was processed using the TSI model IFA755 Digital Burst Correlator signal processors which were controlled using TSI's FIND software. The signal processors were operated in random mode and velocity bias correction using residence time weighting was used for the LDV data.

The energy spectra and the integral length scales were measured with a TSI Model 1210-20 single sensor hot-wire of length, l_w = 1.5 mm, and diameter, d_w = 4 μm. The hot-wire sensor had a frequency response of 100 kHz at 20 m/s, but the analog output was filtered at 10 kHz. Hot-wire data was acquired with a National Instruments AT-MIO-16E-2 analog-to digital board installed in a Dell Pentium90 computer. Data acquisition and analysis was controlled using National Instruments LABView software. Vertical and spanwise length scales, using a two-point correlation, were measured in the development of the turbulence generator. For two-point correlation measurements, synchronization of the LDV and hot-wire data within 20 μs was achieved using a TSI Model DL100 Datalink Interface. Two-point LDV and hot-wire measurements were also used to verify that Taylor's hypothesis was valid in the constant area test section for turbulence levels of 20%.

Static pressure measurements were made around the turbine airfoil in which the taps were connected using flexible tubing to two scani-valves with each capable of measuring 24 channels (giving a total of 48 channels). One scani-valve was connected to a pressure transducer having a differential pressure range up to 0.5 in. H_2O (for use near the stagnation region) and the other scani-valve was connected to a pressure transducer having a differential pressure range up to 2 in. H_2O (for use in the downstream region of the vane). Voltages were read using the National Instruments AT-MIO-16E-2 analog-to-digital board and controlled using LABView software.

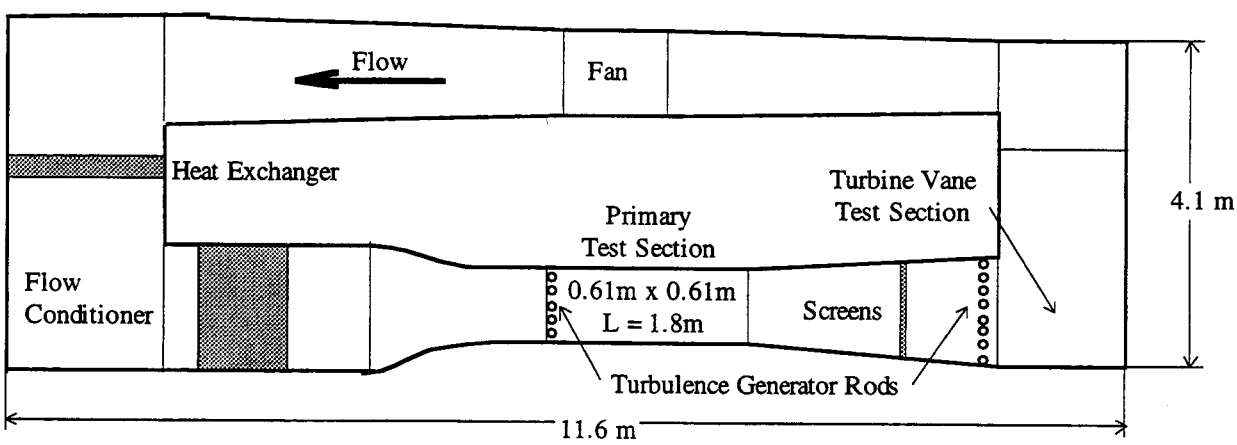

Fig. 1 Schematic of the wind tunnel facility showing the primary test section where the turbulence generator was developed and the corner vane test section where the vane tests were completed.

The uncertainty in the Reynolds number determination was calculated using the root mean square method. Close to the stagnation point, the uncertainty is estimated to be about 13%. This high value results mainly from the uncertainty in the pressure measurement which had to be conducted for pressure differences of less than 3 Pa. Downstream of the leading edge region, the uncertainty in Reynolds number decreases quickly and reaches values of less than 2% at a surface streamwise distance of about s/C = 0.13. The uncertainty, based on a 95% confidence interval, in the mean velocity is 1.7% while the uncertainty in the streamwise rms levels is 2%. The repeatability of the turbulent length scales at a TI = 20% was within 3%.

High Freestream Turbulence Generator Development

Turbulence levels exiting the gas turbine combustor are of the order of 20% and, therefore, generating realistic turbulence levels is an essential part of simulating the flowfield around an actual turbine vane. As discussed earlier, the heat transfer is a function of both the turbulence levels and the length scale of freestream turbulence. In order to fully understand the effect of each of these parameters it is necessary to be able to vary one independent of the other. Previous high turbulence studies have been for a range of turbulence levels that had no control over the length scale with the exception of the work done by Ames (1994 and 1996) as discussed earlier, who had two length scales at a turbulence level of 8%. The specific goals for the design of the turbulence generator were to provide very high turbulence levels (20%) over a range of length scales with uniformity of the mean velocity and turbulence levels within ±5%. Note that development of the turbulence generator was carried out in the square 61 cm by 61 cm primary test section of the wind tunnel. The following paragraphs will describe the initial testing and the final design of the turbulence generator with more detailed information given in Sauer and Thole (1996).

The preliminary design of the turbulence generator was based on the study of Sahm and Moffat (1992) who used an array of single hollow tubes with jet injection at $\alpha = \pm 30°$ to the mainstream. The high turbulence levels were generated by interaction between adjacent high velocity jets and the recirculation region formed behind the grid elements. Using Sahm and Moffat's idea, a turbulence generator using two tubes placed next to each other was tested. Again, this geometry was not a grid, but rather active tube pairs in a crossflow. The tube pair allowed easy adjustment of jet injection angle by rotating the tubes. The capabilities of this design were documented for a variety of parameters namely the total plenum pressure, jet injection angle (α), vertical spacing of the jet holes (s_v) and lateral spacing of the turbulence generator elements (s_L). Tests showed that this design was capable of producing high turbulence levels, but the uniformity of the flowfield was very poor for our large cross-sectional wind tunnel area.

Although the preliminary design was found to have mean velocity uniformities for the large test section greater than ±10%, the experiments gave valuable insight into how the various parameters affected the turbulence generation. Acceptable mean velocity uniformities were considered to be ±5%. For example, results for jet injection angle of $\alpha = \pm 30°$ and ±15° showed that the larger angle caused vigorous interaction between the jets in a region closer to the turbulence generator, resulting in higher turbulence levels. Another parameter which was identified to be important was the ratio of injected mass flux to the mainstream mass flux (MFR). The MFR is defined as the following:

$$\mathrm{MFR} = \frac{\rho_j A_j U_j}{\rho_\infty A_\infty U_{\infty,\mathrm{upstream}}} \qquad (1)$$

Note that the freestream velocity, $U_{\infty,\mathrm{upstream}}$ is the velocity upstream of the turbulence rods and U_j is the velocity calculated using choked conditions and a discharge coefficient of unity. While decreasing the MFR made the mean flowfield more uniform it lowered the turbulence levels. The same effect was observed with the lateral and/or vertical spacing with smaller spacing resulting in lower turbulence levels and a more uniform flowfield.

Although the preliminary design showed promise in generating high levels of turbulence, the streamwise momentum flux added by the jets caused non-uniformities in the mean flow field greater than ±10%. Preliminary tests also showed that while high turbulence levels could be achieved with upstream injection only or downstream injection only, the flow uniformity was quite poor. For our particular geometry, the upstream injection yielded higher turbulence levels and higher flow non-uniformities than did the downstream injection. Therefore, the final design was based on reducing the streamwise momentum flux by simultaneously injecting in the upstream and downstream direction.

Figure 2 shows a schematic of the final design of the turbulence generator having simultaneous upstream and downstream injection. The generator elements are hollow aluminum tubes with a wall thickness of 1 mm and an outer diameter of D = 1.27 cm. The jet holes are of diameter, D_{jet} = 1.5 mm and are vertically spaced s_v/D = 2.4 apart. The lateral spacing between the elements is adjustable. The turbulence generator elements are supplied with compressed air at nominally 140 kPa (gage) from a plenum chamber giving choked conditions for the jet, which is similar to Sahm and Moffat's (1992) design. For each condition tested, the plenum to back pressure ratios were above that for choked conditions and the mass flux ratio was set by varying the plenum pressure for the injection jets. The design of the turbulence generator is such that it can be installed at any desired location in either the primary or secondary test sections of the wind tunnel. For the turbulence generator developmental tests given in this paper, the wind tunnel fan speed was set to insure that the mean velocity downstream of the turbulence generator was between 8 m/s < U_∞ < 9 m/s. For the stator vane tests, these velocities were lower at U_∞ = 6.5 m/s.

Figure 3 gives the turbulence level decays for the various tube spacings and MFRs that were tested with the simultaneous upstream and downstream jet injection as compared with grid generated turbulence (Baines and Peterson, 1951). Note that the streamwise distance for the grid study is normalized using bar width and the streamwise distance for the active grid study is normalized using the rod diameter. Although turbulence measurements upstream of the x/D = 39 are indicated on this plot, it is quite probable for some cases that the mean flow uniformity did not meet the requirement of ±5% upstream of x/D = 39.

In general, turbulence levels for the active grid are much higher than the passive grid. Increasing the MFR results in higher turbulence levels. All of these results indicate the exiting jet plays a major role in generating the turbulence. Note that a larger effect of the MFR occurs at a lateral tube spacing of s_L/D = 9.6 than at s_L/D = 15.9. This large MFR effect for a spacing of s_L/D = 9.6, which is to significantly reduce the turbulence levels at the lower MFR, may be attributed to the rod elements becoming more dominant that the jets.

A comparison of the turbulence decay for the active grid with the passive grid was done using $u'/U_\infty = A\,(x/D)^n$. The exponent for the passive grid was n = -0.714 and for the active grid, depending on spacing and MFR, it ranged between -0.89 < n < -0.60 with the faster turbulence decay occurring at higher MFRs and smaller lateral tube spacings.

Based on the concept that the lateral jet spacing could play a significant impact on the length scale, the lateral distance between the rods

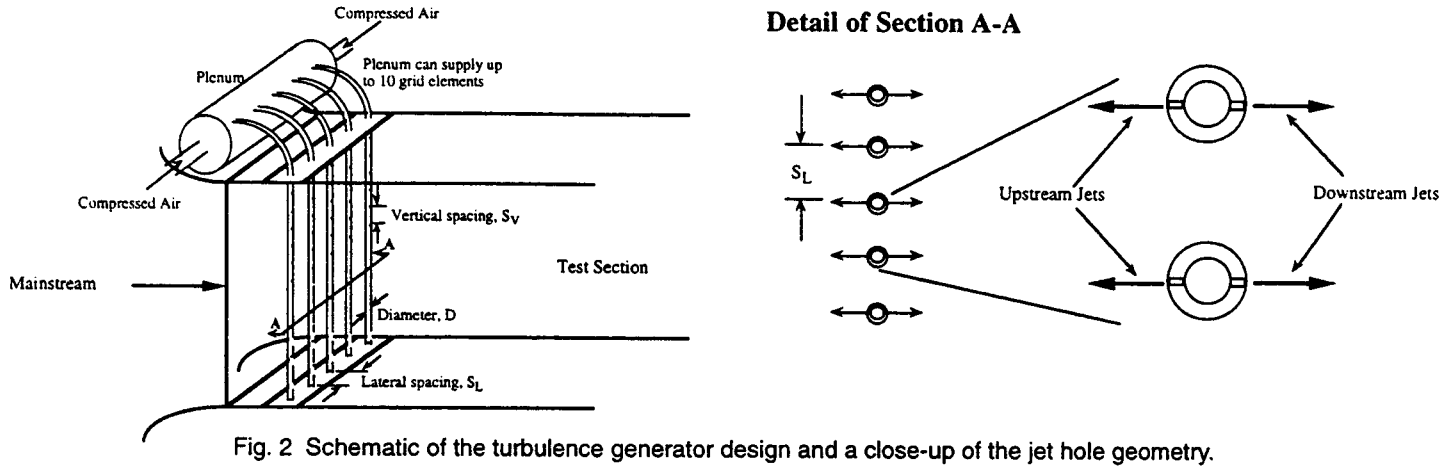

Fig. 2 Schematic of the turbulence generator design and a close-up of the jet hole geometry.

were changed and the integral length scales were measured, as shown in Figure 4. In fact, there is a significant change in the length scales for the different rod spacing with the largest length scale occurring at the widest rod spacing. The range of length scales is between $2.1 < \Lambda_x/D < 4.2$ at a turbulence level of nominally TI = 20%. Note for the MFR = 3.2% case, the TI = 20% at a streamwise distance of x/D = 60 as opposed to the other cases where TI = 20% at nominally x/D = 40. That means to achieve the very large length scale, a larger distance downstream of the generator is required. Tests indicated that when the rod spacing was increased beyond $s_L/D > 15.9$, the flow uniformity was poor and with ratios smaller than $s_L/D < 6.9$, a limit in the minimum length scale was attained. Similar to the turbulence levels, at a spacing of $s_L/D = 9.6$ there was a major influence of the MFR in that the length scales were reduced to sizes close to the rod diameter at the lower MFR = 2.3%.

Several tests were conducted to determine the effect of the MFR and the lateral spacing of the hollow tubes on the mean flow uniformity. Table 1 describes the results for these tests. For each of the different lateral spacings turbulence levels of nominally TI = 20% could be achieved by adjusting the mass flux ratio and still maintain a mean flow uniformity of $\sigma_{Vel}/U_{av} < 6\%$.

Table 1. Effect of Lateral Spacing for the Active Rods

Active Rods	3		5		7	10
s_L/D	15.9	15.9	9.6	9.6	6.9	4.8
MFR (%)	2.5	3.2	2.3	3.5	6.0	8.2
U_{av} (m/s)	9.0	9.3	8.9	8.8	8.7	8.6
σ_{Vel}/U_{av} (%) at x/D = 39	5.6	6.0	3.6	4.4	4.2	3.3
TI_{av} (%) at x/D = 39	22.2	29.9	11.4	19.1	20.2	16.3
σ_{Tu}/Tu_{av} (%) at x/D = 39	7.1	5.8	6.2	3.5	3.2	4.5

Stator Vane Description

A modern, first stage stator vane, having a geometry provided by Pratt & Whitney, was scaled up by a factor of nine and installed into the corner of the large recirculating wind tunnel as previously described in this paper. The geometrical and operational conditions for the stator vane are given in Table 2. Figure 5a shows the geometry of the vane in which the dimensions have been normalized using the chord length and Figure 5b shows a schematic of the corner test section.

In this particular study, close attention was given to matching the Reynolds number distribution that occurs during operation. A two-di-

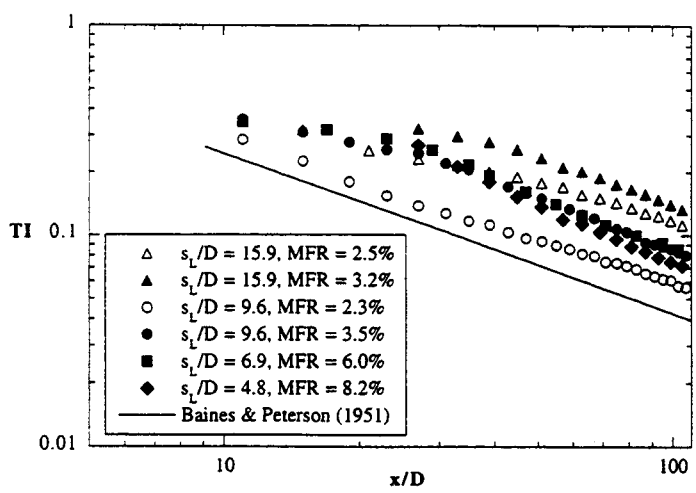

Fig. 3 Turbulence decay rates for different rod spacings and mass flux ratios (MFRs) using the turbulence generator in the primary test section.

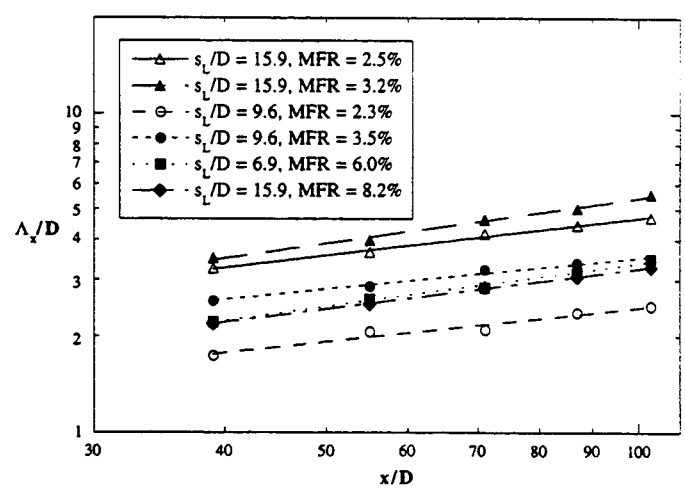

Fig. 4 Turbulent integral length scales for different rod spacings and mass flux ratios (MFRs) using the turbulence generator in the primary test section.

mensional, inviscid analysis using FLUENT (refer to FLUENT User's Guide, 1996) was completed to design the test section for the first stage stator vane. An inviscid analysis was done since it allowed a more reasonable number of computational cells and run-times than a fully viscous solution which requires resolving the boundary layer. The design consisted of a central vane with actual solidity (chord-to-vane spacing) and chord-to-span ratios matched. To match the chord-to-span ratio, a contraction was installed in the diffuser just upstream of the stator vane as discussed above. Downstream of this contraction, both side walls approaching the central vane had a suction slot that fed into a plenum. This suction was controlled using a blower that is in an external flow loop and was designed to remove any side wall boundary layers. On the inner side wall (on the pressure side of the central airfoil) and downstream of the suction slot, another vane leading edge was installed with the stagnation point 5 cm off the side wall. Downstream of the side wall vanes were adjustable tailboards that could be used to insure the trailing edge conditions were met. The outer wall (suction side of the airfoil) started with a leading edge geometry that extended 25% of the chord length which was then attached to a flexible wall. The flexible wall was adjustable to insure engine Reynolds numbers could be achieved. For engine conditions, transonic Mach numbers are achieved which are not matched in these studies. As a result of compressible flow conditions, changes in the static temperature occur which in turn affects the viscosity. Slight adjustments in the flexible side walls were made to accommodate those changes in viscosity and still match the Reynolds number with an incompressible flow where the temperature remains constant.

The vane itself, as well as the side wall leading edges, were constructed using 5.1 cm thick polystyrene pieces that were cut using a heated wire traversed along templates. The total span of the vane was 54.9 cm which was achieved by stacking several of these polystyrene pieces together. The inside of the vanes were cut out such that the wall thickness was 2.54 cm. Small pressure taps, made from brass tubes having an

Table 2. Geometrical and Flow Conditions for Stator Vane

Actual chord length	6.60 cm
Scaling factor	9
Scaled-up chord length	59.4 cm
Chord-to-vane spacing	1.30
Chord to span	1.08
Exit Reynolds number	1.1×10^6
Flow inlet angle	0°
Flow exit angle	78°

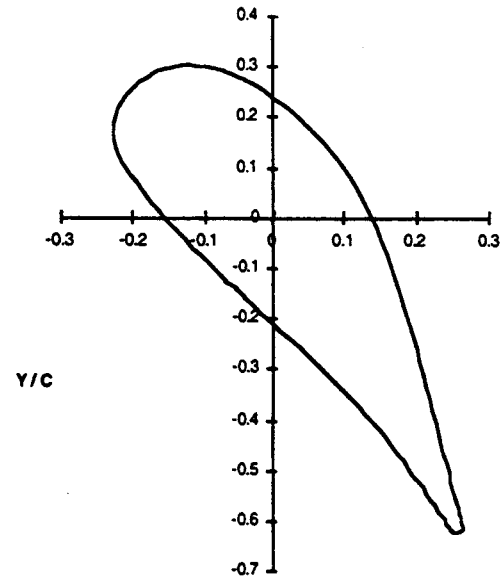

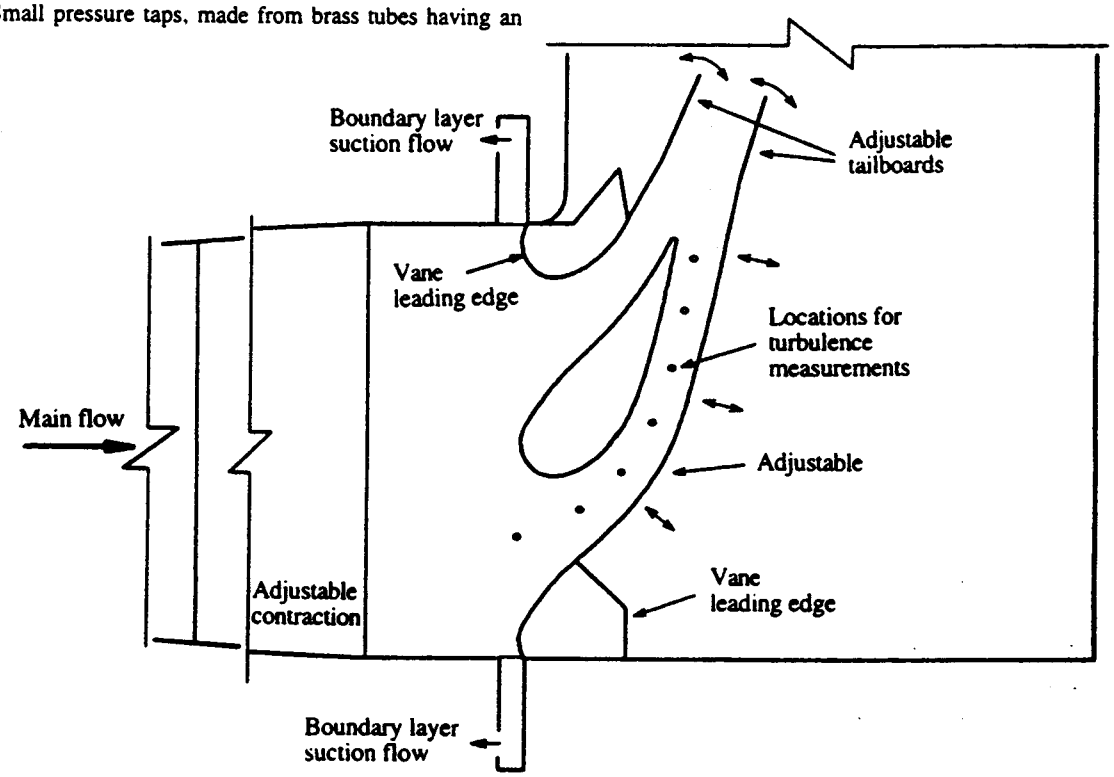

Fig. 5a,b Stator vane geometry and schematic of stator vane installed in the corner test section.

inner and outer diameter of 0.876 mm and 1.588 mm, respectively, were inserted between the polystyrene pieces. A thin sheet (0.03 mm) of mylar was then placed over the entire model and heated with an air gun that allowed a shrink fit of the mylar to the surface producing an aerodynamically smooth surface. Future surface heat transfer tests will be conducted by placing a thin stainless steel foil on the outside of the vane with a current passing through. A total of 37 pressure taps were placed along the blade surface in the center of the vane as well as across the span at several streamwise locations. In addition, there were a number Figures 6a and 6b show the Reynolds number and acceleratation distributions for the vane. The measured, values predicted by FLUENT, and predicted by an inviscid calculation for engine operating conditions are compared. Good agreement is noted in all of the comparisons. On the Reynolds number plot, the pressure taps throughout the span of the central airfoil agreed well with those measured in the center of the airfoil span. There is very good agreement to within 4.5% in the actual, predicted, and measured Reynolds number distributions. Those values given for the inviscid calculation for engine operating conditions were computed by Pratt and Whitney. In the past, predictions similar to those given in Figure 6a for engine operating conditoins with no shocks or separations, have shown good agreement with measured values (Johnson, 1997).

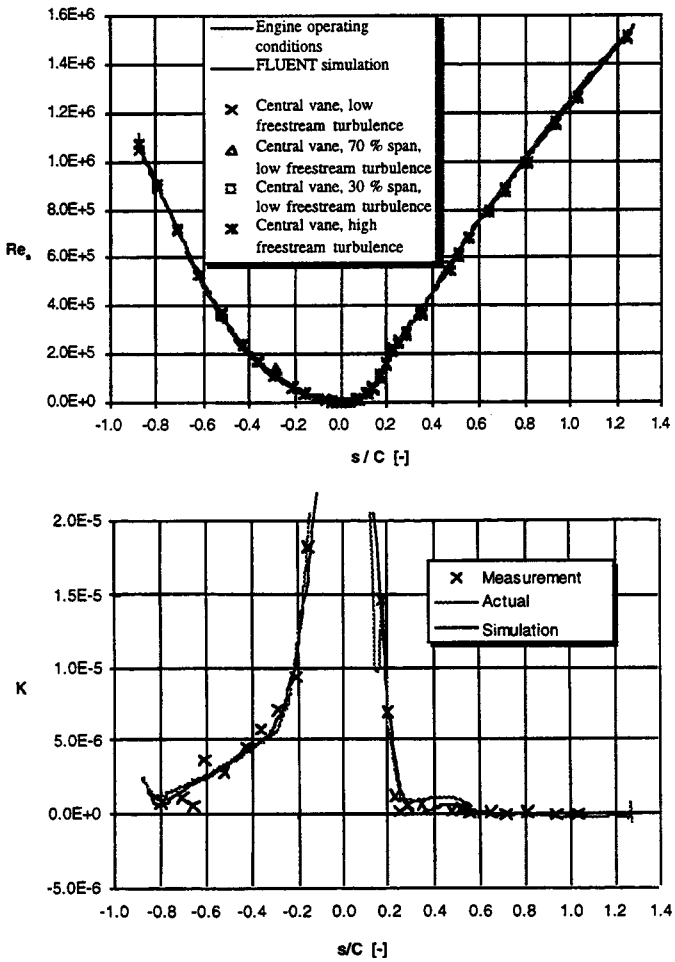

Fig. 6a,b Reynolds number and acceleration parameter comparisons between operating engine, predicted and measured distributions.

Turbulence Measurements in Stator Vane Passage

As discussed earlier, one of the goals of this paper was to compare the behavior of turbulence levels and length scales inside the vane passage with those in the constant area test section in which many high freestream turbulence studies take place. For this purpose, the turbulence generator elements were installed at x/D = 40 upstream of the stagnation location on the center blade. The plenum pressure, was kept fixed at 140 kPa (gage) in order to insure choked flow conditions for the jets. The tunnel velocity was adjusted such that a vane exit Reynolds number of Re = 1.1×10^6 was achieved. In order to achieve a wide range of length scales, lateral spacings of s_L/D = 15.9 and 6.9 were tested at a MFR = 4.4% and 10.1%, respectively. The above operating conditions resulted in much higher values of MFR as compared with those for the primary test section. For purposes of this paper, the turbulence generator was used as is and measurements of length scale and turbulence level were made in the vane passage for two lateral spacings.

Figure 7a shows the variation of turbulence levels in the vane passage. The measurement locations, which took place along a center streamline, are indicated on Figure 5b. Note that the last two data points were taken downstream of where the trailing edge of the neighboring vane would occur in a real gas turbine engine. Although these last two data points may be affected by the outer flexible wall in our simulation, the length scale data indicate that the turbulent scales are only one-third of the total passage width indicating that there would be only a slight effect. The results presented in Figure 7a are plotted in terms of distance from the turbulence generator to allow a direct comparison with data from the primary test section study. Turbulence levels at x/D = 39, which is at the inlet of the vane passage, show good agreement with those seen for the constant area test section. Inside the vane passage, on the other hand, there is a very rapid decrease in turbulence levels. This rapid decrease was also reported by Ames (1994) who described the decrease as an attenuation of the streamwise fluctuations and not a decay since the streamwise dissipation rate remained fairly constant through his turbine vane passage. The attenuation is caused by a strong acceleration and straining of the flow, as was shown by the acceleration parameter, in the leading edge region. Ames (1994) also reported increases in the velocity fluctuations in both the lateral directions.

Length scale results for the vane passage are shown along with those from the primary test section in Figure 7b. In order to allow a direct comparison, the length scale has been normalized by the diameter, D, of the turbulence generator elements. For s_L/D = 6.9, the length scale at the inlet of vane passage shows very good agreement with that for the primary test section. The length scale for s_L/D = 15.9 however, is much larger than its counterpart for the primary test section. This is due to the high value of MFR used for the vane passage measurements which has a big effect for wider element spacings as was shown from the constant area tests. The length scale for s_L/D = 15.9 does not show much change until x/D = 50 and decreases rapidly further inside the vane passage. With a smaller initial length scale, as with s_L/D = 6.9, length scales grow until x/D = 60 before decreasing. Both cases show an increase towards the exit of the vane passage which is consistent with a wider passage.

Though the above length scale results served the purpose of illustrating differences between the two test sections, they were normalized using parameters which did not include any information about the vane passage. As the flow inside the vane passage is constrained, it is reasonable to assume that length scales inside the passage are governed by the geometry of the vane. Therefore, length scales were normalized by the passage width to see how they grow with respect to the vane passage. The turbulence levels and length scale results relative to the turbine vane

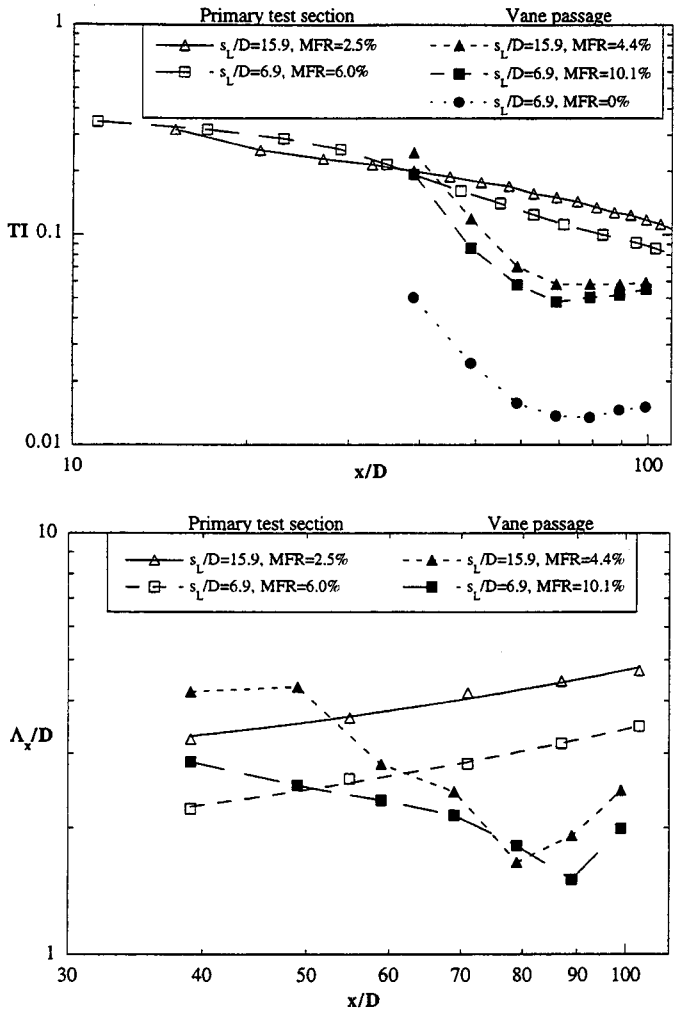

Fig. 7a,b Comparison of turbulence levels and integral length scales in vane passage with those in the primary test section.

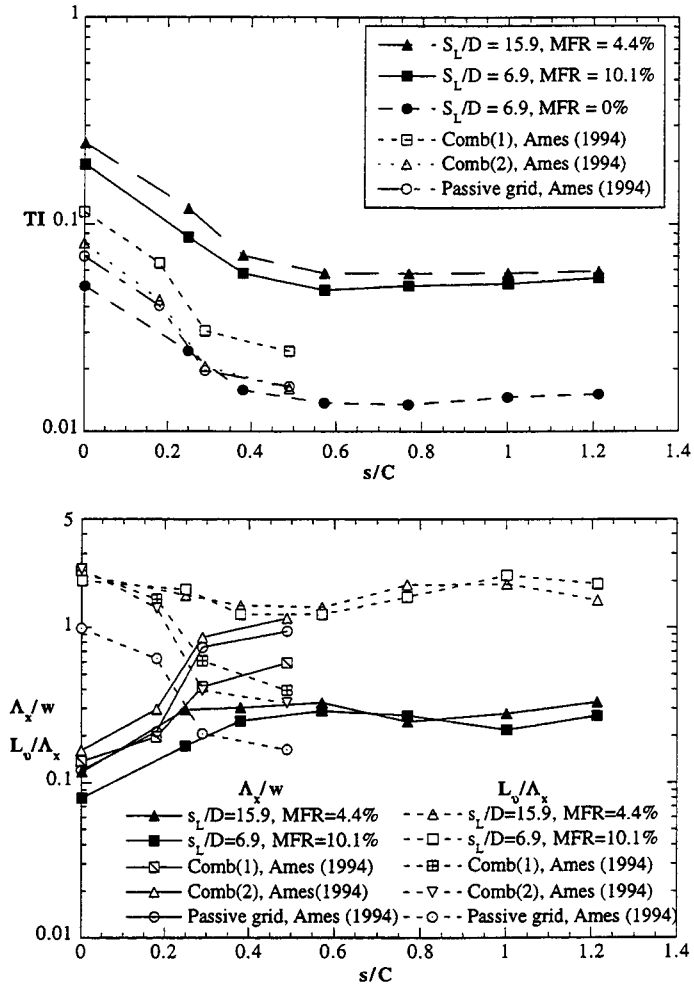

Fig. 8a,b Scaling of turbulence levels and integral length scales in vane passage with those in the literature.

are shown in Figures 8a and 8b. Figure 8a shows that whether or not the inlet turbulence level is high, using the active elements, or is low, using the passive elements with no blowing, there is the same relative initial decrease in turbulence level. For the data presented in this paper, the decrease in turbulence levels are not as rapid as those presented by Ames (1994) because of the smaller ratio of the strain rate time scale (1 / dU/dx) to that of the turbulence (L_u/u'). Our data has a strain rate time scale of 15 ms and a turbulence timescale of nominally 55 ms, as compared to Ames (1994) who had 1.7 ms and 6-17 ms, respectively. For both the active and passive elements, the turbulence intensity decreases by a factor of four over a streamwise distance of the first 40% of the chord length. Note that the strain rate timescale starts to rapidly increase at s/C = 0.4 (as also indicated by the acceleration parameter in Figure 6b) such that it becomes larger than the turbulent timescale thereby not affecting the turbulence decay. Once the strain rate timescale becomes larger than the turbulent time scale, both the streamwise turbulence level and length scales become nearly constant. Figure 8b shows that even though the turbulent length scales are quite different coming into the turbine vane passage, the length scales have a similar behavior for the streamwise locations beyond the s/C = 0.4 position.

Energy spectra of the streamwise velocity fluctuations are shown in Figure 9 for both the large and small inlet turbulence length scales at three different positions. Note that these spectra have been vertically shifted to allow the measurements to be put on a single plot. Also shown in Figure 9 are lines indicating a -5/3 and -1 slope. The -5/3 slope best represents isotropic, homogeneous tubulence while the -1 slope represents wall-bounded turbulence. At the first position, s/C = 0, the turbulence is best represented by the -5/3 isotropic decay. Althought a -5/3 slope still represents the inertial subrange at s/C = 0.6, the spectra begins to show the effects of the passage walls as seen by a small region with a -1 decay. At s/C = 1.2, a significant portion of the energy spectra, corresponding to the large scales, is represented by the -1 slope. Note that a larger region of a -1 slope occurs for the larger length scale case (s_L/D = 6.9). This effect was similarly reported by Ames (1994), who discussed the wall influences on the large length scales.

Conclusions

A turbulence generator capable of generating very high turbulence levels (20%) and with mean and turbulence flow field uniformity of ±5% was successfully developed for a wind tunnel having a large cross-sec-

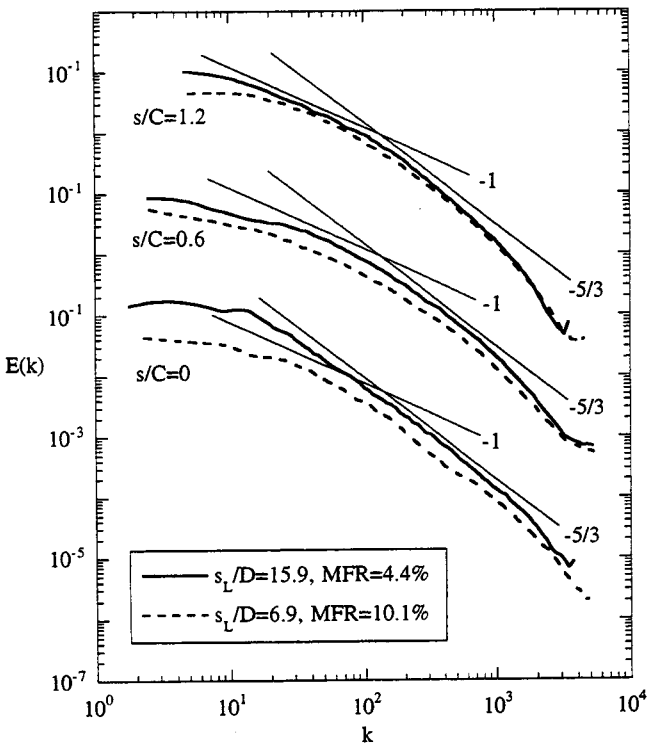

Fig. 9 Turbulent energy spectra for streamwise velocity fluctuations in the turbine vane passage.

tional area. A key feature of this turbulence generator was that it allowed independent control of the length scale which ranged between 2.9 cm < Λ_x < 5.5 cm at a TI = 20% for the constant area test section where it was developed. The turbulence generator design used an array of active elements in which choked jets injected in both upstream and downstream directions. Detailed documentation of the turbulence levels and length scale characteristics were presented for different lateral spacings and injection ratios. This development took place such that the generator could also be applied to a stator vane simulating realistic conditions.

A modern-day stator vane, with the geometry provided by Pratt & Whitney, was scaled up by a factor of nine and installed into a corner test section of the wind tunnel. A two-dimensional, inviscid analysis was used to design the test section to insure that actual Reynolds numbers were matched. The design consisted of a central vane and two adjacent leading edge geometries that were followed by flexible walls. The walls were slightly adjusted to account for the temperature variation on viscosity which occurs in actual engine conditions and does not occur in the scaled-up model. The measurements showed good agreement with the actual engine Reynolds numbers.

Using the turbulence generator upstream of the stator vane, a range of length scales at a TI = 20% occurred between 2.9 cm < Λ_x < 5.4 cm. Measurements of turbulence levels and length scale in the stator vane passage, using the turbulence generator design, showed significant differences in the streamwise development as compared to results from the constant area test section. The turbulence intensities decrease and the turbulent length scales grow rapidly over a streamwise distance of s/C = 0.40. These rapid changes are attributed to the strong acceleration which occurs over the first 20% streamwise distance of the passage. Both the turbulence intensities and length scales remain unchanged for the remainder of the streamwise distance through the passage. These results are consistent with published heat transfer data that show large effects of freestream turbulence near the leading edge region as compared with the trailing edge region. These past studies indicate a necessity for further studying the effects of length scale and turbulence intensity in the leading edge region of vane passages.

The development of this new facility was to allow for detailed boundary layer measurements along a modern day, stator vane. The particular emphasis of future studies for this facility will be to determine the effects that freestream turbulence and turbulent length scales have on the boundary layer development and surface heat transfer along an airfoil.

Acknowledgments

Thanks to P. Dean Johnson, Pratt & Whitney, for providing the stator vane characteristics.

References

Ames, F. E. and Moffat, R. J. (1990) "Heat Transfer with High Intensity, Large Scale Turbulence: The Flat Plate Turbulent Boundary Layer and The Cylindrical Stagnation Point," Stanford University, Report No. HMT-44.

Ames, F. E. (1994) "Experimental Study of Vane Heat Transfer and Film Cooling at Elevated Levels of Turbulence," NASA Contractor Report 4633.

Ames, F. E. (1995) "The Influence of Large Scale High Intensity Turbulence on Vane Heat Transfer," ASME No. 95-GT-21, Houston, Texas.

Baines, W. D. and Peterson, E. G. (1951) "An Investigation of Flow Through Screens," *Transactions of the ASME*, vol. 73, pp. 467-480

Comte-Bellot G. and Corrsin S. (1971) "Simple Eulerian Time Correlation of Full- and Narrow-band Velocity Signals in Grid-Generated Isotropic Turbulence," *Journal of Fluid Mechanics* , vol. 48, Part 2, pp. 273-337.

Gad-El-Hak, M. and Corrsin, S. (1974) "Measurements of Nearly Isotropic Turbulence Behind a Uniform Jet Grid," *Journal of Fluid Mechanics*, vol. 62, part 1, pp. 115-143.

Hoffs, A., Drost, U. and Bölcs (1996) "Heat Transfer Measurements on a Turbine Airfoil at Various Reynolds numbers and Turbulence Intensities Including Effects of Surface Roughness," ASME No. 96-GT-169, Birmingham, UK.

Johnson, P. D. (1997) Personal communication.

Koutmos, P. and McGuirk, J. J. (1989) "Isothermal flow in a Gas Turbine Combustor — a Benchmark Experimental Study," *Experiments in Fluids*, Vol. 7, p. 344.

Maciejewski P. K. ; Moffat R. J. (1992) "Heat Transfer With Very High Free-Stream Turbulence: Part I-Experimental Data," *ASME J of Heat Transfer*, vol. 114, pp. 827-839

MacMullin, R., Elrod, W., and Rivir, R. (1989) "Free-Stream Turbulence From a Circular Wall Jet on a Flat Plate Heat Transfer and Boundary Layer Flow," *ASME J of Turbomachinery*, vol. 111, pp. 78-86

Sahm, M. K. and Moffat, R. J. (1992) "Turbulent Boundary Layers with High Turbulence: Experimental Heat Transfer and Structure on Flat and Convex Walls," Report No. HMT-45, Stanford University.

Sauer, J. and Thole, K. A. (1996) "Development of a High Freestream Turbulence Generator," Report 96-1, University of Wisconsin.

Tan-atichat, J., Nagib, H. Drubka, R. (1980) "Effects of Axisymmetric Contractions on Turbulence of Various Scales," NASA CR 165136.

Tass, Y. and Kamotani, Y. (1975) "Experiments on Turbulence Behind a Grid with Jet Injection in Downstream and Upstream Direction," *Physics of Fluids*, vol. 18, no. 4, pp. 411-414.

Thole, K. A. and Bogard, D. G. (1994) "Generating High Freestream Turbulence Levels," *S*, vol. 17, pp. 375-380.

Young, C. D., Han, J. C., Huang, Y., and Rivir, R. B. (1992) "Influence of Jet-Grid Turbulence on Flat Plate Turbulent Boundary Layer Flow and Heat Transfer," *ASME J. of Heat Transfer*, Vol. 114, pp. 65-72.